Satellite Monitoring of the Global Ocean Surface During 1987–1989

David Halpern

Abstract

Long-term simultaneous global coverage of AVHRR sea surface temperature, SSMI surface wind speed, GEOSAT sea surface height, and ARGOS buoy drift began in 1987. Methodology to create annual atlases of monthly mean distributions is described.

1 Introduction

Progress in climate research depends on the availability of a variety of geophysical data sets to describe the boundary conditions and forcing functions of the climate system. The importance of long-period global data sets is highlighted in the U.S. National Aeronautics and Space Administration (NASA) Earth Observing System and the U.S. Committee on Earth and Environmental Sciences Global Change Research Program. The unique perspective from space provides the opportunity for observations well suited for the global ocean, which is an essential component of the climatic system and which remains severely undersampled.

Stommel and Fieux (1978), in their guide to oceanographic atlases, stated that "the oceanographic atlas is one of the main tools of the oceanographer". Because of the scarcity of oceanographic data, very few atlases cover the world ocean, and none provide monthly mean distributions for a particular year. Several years of monthly mean data are necessary to analyze the seasonal cycle and interannual variations.

Since about ten years ago, substantial advances in remote and in situ techniques to record temperature, sea level, horizontal current, and surface wind have helped define annual cycles and interannual variations. Innovative ideas of how the ocean and atmosphere are coupled together occurred in parallel with new instrumentation. Three examples are El Niño Southern Oscillation, the ocean-atmosphere flux of carbon, and the relationship between global sea surface temperature and precipitation over Africa.

Monthly mean distributions of geophysical variables, which cover the globe or a large-scale region like an ocean basin, are becoming de rigueur. Although both satellite- and ground-based recording systems provide essential information for global climate studies, satellite-borne instrumentation yields unprecedented spatial and temporal coverage of the global ocean. The production of a continuing

series of annual atlases was initiated in 1990 to meet the challenge of a visually attractive display of simultaneous monthly mean global oceanographic variables for education and research. Each atlas contains color displays of monthly mean distributions of satellite measurements for a 1-year interval. Satellite-derived surface wind speed, sea surface temperature, buoy drift, and sea surface height variation are described. Data limitations restricted the inclusion of all measurements in each atlas (Table 1). Each atlas also displays surface wind vector components, which were computed by a numerical forecast-analysis system.

2 Satellite-Derived Oceanographic Measurements

2.1 SSMI Wind Speed

The special sensor microwave imager (SSMI) is a 7- channel, 4-frequency, linearly polarized, passive microwave radiometer flown on the U.S. Air Force's Defense Meteorological Satellite Program (DMSP) F8 spacecraft in a circular sun-synchronous near-polar orbit at an altitude of approximately 860 km and an orbit period of 102.0 min. The orbit has an ascending (south-to-north) equatorial crossing at 0613 local time. The first SSMI of a series of ten was launched on 7 July 1987. The nearly 1400-km swath of SSMI produces complete coverage between 87°36'S to 87°36'N every 3 days. Each of the 7 separate passive radiometers measures naturally occurring microwave emissions from land, water and ice surfaces and from the intervening atmosphere. The SSMI receives both vertical and horizontal linearly polarized radiation at 19.3, 37.0 and 85.5 GHz and vertical only at 22.2 GHz.

The emitted microwave radiometer at the ocean surface is affected by roughness of the sea surface, which is correlated with the near-surface wind speed. Each atlas uses the Wentz (1989) surface wind speed data product. The Wentz (1989) algorithm relates wind speed at 19.5-m height (w, m s^{-1}) to the 37-GHz brightness temperatures, which are computed from the SSMI 37-GHz horizontal and vertical polarized radiance measurements, and to the radiative transfer and absorption between the sea surface and SSMI. The SSMI wind speed referenced to 10-m height is equal to 94.3% of w (Wentz, 1989).

The Wentz (1989) GDR contains wind speed values in nonoverlapping areas of 25 km x 25 km, which are arrayed across the 1394-km SSMI swath width. SSMI wind speeds within nonoverlapping 1/3° x 1/3° squares were arithmetically

wind speed represented the arithmetic mean of several values. The total number of individual SSMI values was low in July 1987 and January 1988 (Figure 1B) because the instrument was not operated the entire months. The December 1987 data set ended on 4 December (Table 1) because of a 40-day off-period to avoid possible damage of the SSMI by increased heating of the bearing and power transfer assembly (Hollinger et al., 1990). During subsequent winters, the DMSP spacecraft solar arrays were repositioned so that the SSMI was not turned off.

The SSMI accuracy specification for wind speed retrievals under rain-free conditions is ± 2 m s-1 rms over the range 3-25 m s-1. Wentz (1991) compared SSMI wind speeds with a National Oceanic and Atmospheric Administration (NOAA) National Data Buoy Center moored buoy wind data set prepared by Goodberlet et al. (1990), and found differences of zero bias and 1.6 m s^{-1} rms. Model functions different than Wentz' (1989) physically-based algorithm exist. The Environmental Research and Technology (ERT) algorithm for SSMI surface wind speed did not meet the accuracy specification (Goodberlet et al., 1990). Bates' (1991) statistical algorithm with brightness temperatures from five SSMI channels had a 1.1 m s^{-1} bias and a 1.8 m s^{-1} rms difference with moored buoy wind measurements at four sites from 5° to 5°N along 165°E. Halpern (in preparation) compared monthly mean Remote Sensing Systems-derived SSMI wind speeds and moored-buoy wind measurements at nearly 50 sites during 1988 and 1989: the root-mean-square (rms) difference was 1.2 m s^{-1}; and for SSMI monthly standard deviations of 1 - 2, 2 - 3, and 3 - 4 m s^{-1}, the average absolute values of the monthly mean difference were 0.6, 0.9, and 1.4 m s^{-1}, respectively.

2.2 GEOSAT Sea Surface Height

On 1 October 1986 the U.S. Navy's geodetic satellite (GEOSAT), which was launched on 12 March 1985, was maneuvered into an exact repeat orbit for oceanographic studies, which was named the Exact Repeat Mission (ERM). Each GEOSAT ERM orbit repeats within 1 km every 17.0505 days. The ground track separation at the equator is about 164 km. Global ERM data exists from 8 November 1986 until September 1989 when both tape recorders on GEOSAT ceased to operate; however, global data coverage was very poor after March 1989.

The technique is complex to convert a radar altimeter's travel time measurement between the satellite and the sea surface into a meaningful estimate of the elevation of the sea surface relative to a reference surface, which becomes the oceanographic signal of interest. The GEOSAT sea surface height data set used in the 1987- and 1988-atlases was based on the Zlotnicki et al. (1990) data product. Along each groundtrack, the environmentally corrected GEOSAT sea surface height relative to the reference ellipsoid, $SSH_{corrected}$, were resampled at fixed latitudes at about every 7 km using a cubic spline. No interpolation was made over a data gap larger than 3 s (≈ 21 km). During each ERM year, the groundtrack was repeated approximately 22 times. For each series of 22 repeats of the groundtracks, the repeated groundtrack with the most resampled $SSH_{corrected}$ values was defined as a reference groundtrack. SSHcorrected differences or residuals, called SSH',

were computed between the reference groundtrack and all other groundtracks within the series. This deleted a 25 m rms uncertainty caused by the geoid (Zlotnicki, 1991). The orbit error was further reduced from 35 cm rms to less than 5 cm rms by fitting a once per revolution (≈ 101 minutes) sine wave to resampled SSH'. The resampled, edited, environmentally corrected, GEOSAT residual sea surface heights are called SSH".

A 2-year (6 November 1986 - 5 November 1988) arithmetic mean SSH" value, <SSH">, was computed at each location where 17 or more SSH" values existed. At sites where the 2-year mean SSH" value was not computed because of insufficient data, SSH" values were deleted from further data processing. Sea surface heights relative to the 2- year mean, η = SSH" - <SSH">, were then computed. All η values with positions within nonoverlapping 1/3° x 1/3° squares were arithmetically averaged in 30.5-day intervals to form the basic monthly data set. The total number of 1/3° x 1/3° monthly-averaged η values decreased slightly from January 1987 to December 1988 (Figure 2A). Each 1/3° x 1/3°-η value represented the arithmetic mean of several η values. The total number of individual η values involved in the creation of each monthly averaged distribution decreased slightly from January 1987 to December 1988 (Figure 2B).

The accuracy of satellite altimeter estimates of sea surface height depends very much on the data processing procedures. Zlotnicki (personal communication, 1992) compared GEOSAT alongtrack data with the Wyrtki et al. (1988) tide gauge data from the Indian and Pacific Oceans. The η values were averaged over a 100-km groundtrack nearest to a tide gauge; this time series is called η100 km. The in situ 1-hour sampled sea level time series was low-passed filtered so that 50 and 95% of the amplitude squared were deleted at 2.5 and 1.7 days, respectively. Each low-passed filtered tide gauge time series was resampled at 17.05 days so that the times were coincident with the η100 km data set; the resampled in situ time series are called SL. Comparison of η100 km and SL time series at during 1987 - 1988 indicated an rms difference of 12.8 cm and the median correlation between the two time series was 0.43.

2.3 AVHRR/2 Sea Surface Temperature

The NOAA satellite platforms (called NOAA-j where j is an integer) are in sun-synchronous orbits at altitudes of 833 or 870 km with ascending equatorial crossings at 0730 or 1400 local time. Since the 1981 launch of NOAA-7, odd-numbered NOAA satellites have a five-channel advanced very high resolution radiometer called AVHRR/2. Even-numbered satellites have a four-channel advanced very high resolution radiometer called AVHRR. The AVHRR/2 scan rate is 360 swaths per min with a total field of view of ± 55.4° from nadir and with an effective ground resolution of 1.1 km at nadir in five coregistered bands. Two spectral channels are in the visible range (0.58 - 0.68 and 0.725 - 1.1 μm) and three in the infrared range (3.55 - 3.93 (i.e., 3.7) μm, 10.3 - 11.3 (i.e., 11) μm, 11.5 -12.5 (i.e., 12) μm). Infrared radiation received by a satellite radiometer is determined primarily by the sea surface emissivity and temperature and by atmo-

spheric transmittance. Atmospheric absorption of emitted radiation at the AVHRR/2 infrared wavelengths is primarily by water vapor, which occurs in the lower levels of the atmosphere. The transmission of emitted radiation through the atmosphere differs for each AVHRR/2 wavelength so that the difference of satellite- measured radiances at two or more wavelengths is independent of atmospheric absorber concentration. For small cumulative amounts of water vapor in the atmosphere, a linear combination of AVHRR/2 infrared radiation measurements recorded at the satellite yields an estimate of sea surface temperature, which is known as multi- channel sea surface temperature (MCSST). Radiance measurements from only cloud-free areas are processed by NOAA into MCSSTs. Very conservative cloud tests, which involve various combinations of the visible and infrared AVHRR/2 data, detect clouds so that cloud-free MCSSTs are computed (McClain et al., 1985); on a typical day, less than 2% of the maximum possible number of MCSSTs are retained.

The atlases contain day-time MCSST data produced operationally by NOAA's National Environmental Satellite and Data Information Service (NESDIS). The procedure is described by McClain et al. (1985). The 1.1-km AVHRR/2 observations are available only within areas containing a downlink ground station to receive high-resolution data transmission. Global AVHRR/2 measurements have an effective ground resolution of 4 km. A computer on board the NOAA spacecraft generates an average radiance for each channel from four 1.1-km elements within each nonoverlapping group of five consecutive 1.1-km measurements along a scan. The day-time MCSSTs archived on NESDIS global retrieval tapes represent the average sea surface temperatures within 8 km x 8 km areas, which would occur at 25-km intervals in a cloud-free environment. The 8-km x 8-km MCSSTs are mapped at the University of Miami's Rosenstiel School of Marine and Atmospheric Sciences (RSMAS) onto a cylindrical equi-rectangular grid of 2048 (longitude) x 1024 (latitude) space-elements (Olson et al., 1988). At the equator the dimension of each space-element is approximately 18 km x 18 km, and geographical coordinates are assigned to the center of the element. RSMAS produces MCSSTs averaged over 7 days. Four consecutive 7-day values are arithmetically averaged to form 28-day mean MCSST values A 1024 x 512 grid was created by computing the arithmetic mean of four 18-km x 18-km MCSSTs adjacent to each other in a 2-dimensional array. The average MCSSTs of 4-element groups, which were independent of each other, represent an approximate 1/3° x 1/3° gridded MCSST data set.

The total number of 1/3° x 1/3° monthly-averaged MCSST values was smallest during June, July, and August, which coincided with intense cloud cover over huge oceanic areas of the middle latitudes of the southern hemisphere, and was highest during December, January, and February (Figure 3A). The range between maxima and minima was more than 25% of the annual mean.

The RSMAS MCSST data set contains the number of 8 km x 8 km values averaged to yield the 2048 x 1024 grid. The total number of 8 km x 8 km values

per month (Figure 3B) was low throughout most of 1987 and 1988 compared to that during 1989.

The coefficients used in the NOAA MCSST algorithm change only as the operational satellite is replaced and on rare occasions when the continuous validation procedure indicates a need for a change. NOAA continuously monitors the performance of the MCSST data product with satellite- tracked drifting buoy sea surface temperature measurements, which are recorded within 25 km and 4 h of the location of the MCSST. During 1987 - 1989, the MCSST was 0.04°C less than the in situ data and the rms difference was 0.7°C for an average of 388 matchups per month throughout the global ocean (Table 2).

2.4 ARGOS Buoy Drift

Since the late 1970s free-drifting buoys have been tracked throughout the world ocean by ARGOS, which is the French navigation system on NOAA polar orbiting satellites. ARGOS buoy drift data were not included in the atlases for 1987 and 1988 because the number of drifting buoys was considered insufficient for a global perspective. Canada's Marine Environmental Data Service (MEDS), which is a Responsible National Oceanographic Data Center (RNODC) for Drifting Buoy Data, continuously acquires ARGOS-tracked drifting-buoy positions trans-

indicated no drogues were attached to any buoys. However, some buoys, particularly in the tropical Pacific Ocean, contained a drogue at 15-m depth but information about the drogue depth was not transmitted on the GTS (D. Hansen, personal communication, 1992). Many drift buoys in the Southern Ocean had no drogue or contained a 100-m nylon line. Caution must be exercised in the interpretation of the 1989 buoy drift as near-surface current because of the unknown status and quality of the buoy and drogue.

2.5 Data Presentation

All data are presented in the annual atlases in the form of color-coded maps. To ease interpretation of features among different parameters, a common color code is used: blues represent low values, reds are high values, yellow and green are in the middle range, white means no data, and black represents land. Data are linearly scaled for color and an incremental color scale represents a contour interval. A single geographical scale is used for all maps. The land mask is the same throughout this report.

The color maps were generated on a Sun™-4 computer using IDL®, which prepared the PostScript® files, and printed on a Tektronix™ Phaser CP Color Printer. All data values are retained in the PostScript® image files. The SSMI images contain 1080 x 540 pixels (picture elements) and the AVHRR images contain 1024 x 512 pixels. All images are plotted on a 5.75-in. x 2.875-in. map. The PostScript® interpreter linearly transforms the size of each pixel within the user image file into a source-image coordinate system, which is compatible with the 300 dot-per-in. resolution of the Tektronix™, to achieve the maximum rendition of the image.

3 Summary

Prediction of the intensity and timing of enhanced greenhouse warming caused by humankind's introduction of radiatively active gases into the atmosphere is heavily weighted with uncertainty. Improvement in prediction of the annual cycle and interannual variations of global variables is necessary to increase reliability of predictions of global warming. An impediment to global coupled ocean-atmosphere models is absence of global oceanographic data sets. The ability to make good use of satellite data is an important consideration.

The need for simultaneous global oceanographic observations has been often stated; perhaps Rennell, in 1822, made the earliest recorded statement (Pollard and Griffiths, 1991), which was followed by Maury (1885). The need for concurrent oceanographic observations remains as significant today as a century ago. Many studies of climate variations require knowledge of monthly mean global surface-oceanographic distributions with minimal amount of aliasing. The annual atlases displays observations from different satellites operated by different agencies. Very little averaging or interpolation of the data was made to retain the fundamental

sampling characteristics of each data set. Deficiencies of current remote sensing systems are easily seen in the atlas maps of data sampling density, which should be especially interesting to developers of new and innovative satellite-borne instrumentation.

Acknowledgements

References

Bates, J.J. (1991) High frequency variability of SSMI- derived wind speed and moisture during an intraseasonal oscillation. *Journal of Geophysical Research*, 96, 3411- 3424.

Bitterman, D.S., and D.V. Hansen (1989) Direct measurements of current shear in the tropical Pacific Ocean and its effect on drift buoy performance. *Journal of Atmospheric and Oceanic Technology*, 6, 274-279.

Brügge, B., and J. Dengg (1991) Differences in drift behavior between drogued and undrogued satellite-tracked drifting buoys. *Journal of Geophysical Research*, 96, 7249-7263.

Geyer, W.R. (1989) Field calibration of mixed-layer drifters. *Journal of Atmospheric and Oceanic Technology*, 6, 333-342.

Goodberlet, M.A., C.T. Swift and J.C. Wilkerson (1990) Ocean surface wind speed measurements of the special sensor microwave imager (SSMI). *IEEE Transactions on Geoscience and Remote Sensing*, 28, 823-828.

Halpern, D., V. Zlotnicki, J. Newman, O. Brown and F. Wentz (1991) An atlas of monthly mean distributions of GEOSAT sea surface height, SSMI surface wind speed, AVHRR/2 sea surface temperature, and ECMWF surface wind components during 1988. JPL Publication 91-8, Jet Propulsion Laboratory, Pasadena, 110 pp.

Halpern, D., V. Zlotnicki, J. Newman, D. Dixon, O. Brown and F. Wentz (1992a) An atlas of monthly mean distributions of GEOSAT sea surface height, SSMI surface wind speed, AVHRR/2 sea surface temperature, and ECMWF surface

wind components during 1987. JPL Publication 92-3, Jet Propulsion Laboratory, Pasadena, 111 pp.

Halpern, D., W. Knauss, O. Brown and F. Wentz (1992b) An atlas of monthly mean distributions of GEOSAT sea surface height, SSMI surface wind speed, AVHRR/2 sea surface temperature, and ECMWF surface wind components during 1987. JPL Publication 92-3, Jet Propulsion Laboratory, Pasadena, 112 pp.

Maury, M.F. (1885) The Physical Geography of the Sea. Harper and Brothers, 274 pp. McClain, E.P., W.G. Pichel and C.C. Walton (1985) Comparative performance of AVHRR-based multichannel sea surface temperatures. *Journal of Geophysical Research*, 90, 11587-11601.

Niiler, P.P., R.E. Davis and H.J. White (1987) Water- following characteristics of a mixed layer drifter. *Deep-Sea Research*, 34, 1867-1881.

Olson, D.B., G.P. Podesta, R.H. Evans and O.B. Brown (1988) Temporal variations in the separation of Brazil and Malvinas Currents. *Deep-Sea Research*, 35, 1971-1990.

Paduan, J.D., and P.P. Niiler (1991) The WOCE/TOGA surface velocity program. ARGOS Newsletter, No. 42, 1-5. (Available from Service ARGOS Inc., Landover, MD 20785)

Pollard, R. and G. Griffiths (1991) James Rennell: The father of oceanography. *Ocean Challenge*, 2 (2), 19- 21.

Stommel, H., and M. Fieux (1978) Oceanographic Atlases. Woods Hole Press, Woods Hole, Massachusetts, 6 pp + 97 charts.

Thomson, R.E., P.H. LeBlond, and W.J. Emery (1990) Analysis of deep-drogued satellite-tracked drifter measurements in the northeast Pacific. *Atmosphere-Ocean*, 28, 409-443.

Wentz, F.J. (1989) User's manual: SSMI geophysical tapes. RSS Technical Report 060989, Remote Sensing Systems, Santa Rosa, California, 16 pp.

Wentz, F. (1991) Measurement of oceanic wind vector using satellite microwave radiometers. Submitted to *Journal of Geophysical Research*.

Wyrtki, K., P. Caldwell, K. Constantine, B.J. Kilonsky, G.T. Mitchum, B. Miyamoto, T. Murphy and S. Nakahara (1988) The Pacific island sea level network. JIMAR 88-137, University of Hawaii, Honolulu, 71 pp.

Zlotnicki, V. (1991) Sea level differences across the Gulf Stream and Kuroshio Extension. *Journal of Physical Oceanography*, 21, 599-609.

Zlotnicki, V., A. Hayashi and L.-L. Fu (1990) The JPL- Oceans-8902 version of GEOSAT   altimetry data. JPL Internal Document D-6939, Jet Propulsion Laboratory, Pasadena, 17 pp + 60 charts.

Table 1. Duration of satellite-derived monthly mean measurements contained in annual atlases. Surface wind speed = S; sea surface height variation = SSH; sea surface temperature = SST; satellite-tracked drifting buoy = BUOY DRIFT. Detailed descriptions of the methodologies used to compute the satellite-derived measurements are given in the references.

Data-Year	S	SSH	SST	Buoy Drift	Reference
1987	Jul-Nov	Jan-Dec	Jan-Dec		Halpern et al.
(1992a) 1988		Jan-Dec	Jan-Dec	Jan-Dec	Halpern et al.
(1991) 1989		Jan-Dec	Jan-Dec	Jan-Dec	Halpern et al.
(1992b) 1990		Jan-Dec	Jan-Dec	Jan-Dec	Halpern et al. (in preparation)
1991	Jan-Dec		Jan-Dec	Jan-Dec	Halpern et al. (in preparation)

Table 2. Annual statistics of the global monthly mean bias and root-mean-square (RMS) difference between daytime MCSST and drifting-buoy SST (DRIBU SST) matchups A matchup occurs when the MCSST was measured within 4 h and 25 km of a drifting-buoy SST. Bias = DRIBU SST - MCSST. (Monthly data courtesy of Dr. E. P. McClain, NOAA NESDIS)

Year	Monthly Average Number of Matchups	Bias °C	RMS Difference °C
1987	234	-0.03	0.7
1988	245	-0.06	0.7
1989	384	-0.02	0.7

Number of Data Grid-Points per Monthly Global Distribution
of SSMI 10-m Height Wind Speed

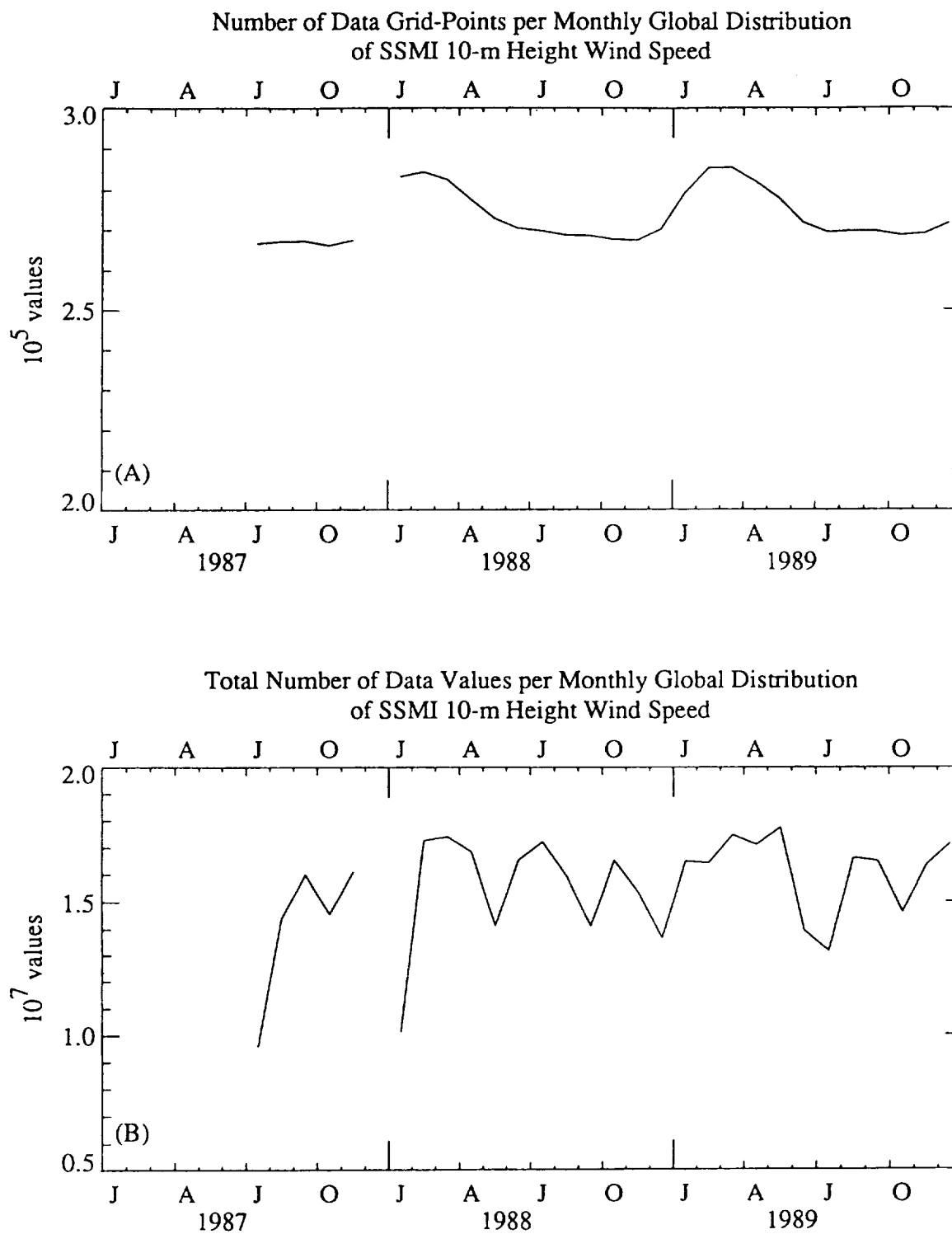Total Number of Data Values per Monthly Global Distribution
of SSMI 10-m Height Wind Speed

Figure 1. Time series of monthly totals of (A) number of 1/3° x 1/3° pixels or picture elements and (B) number of SSMI 10-m height wind speeds.

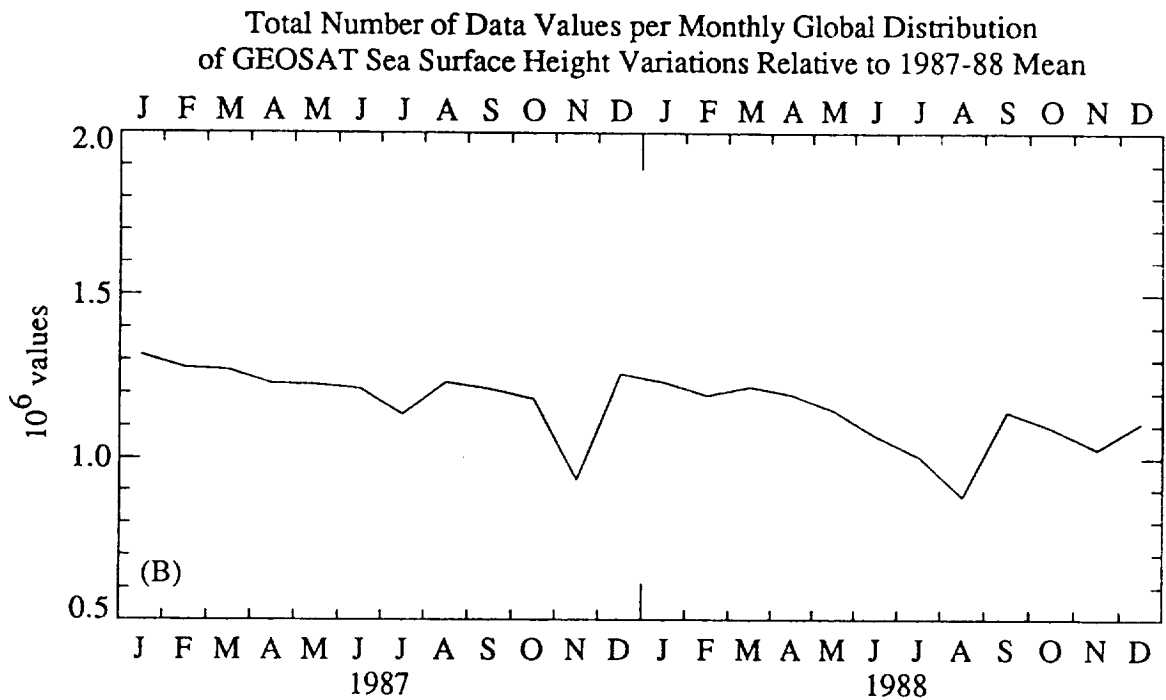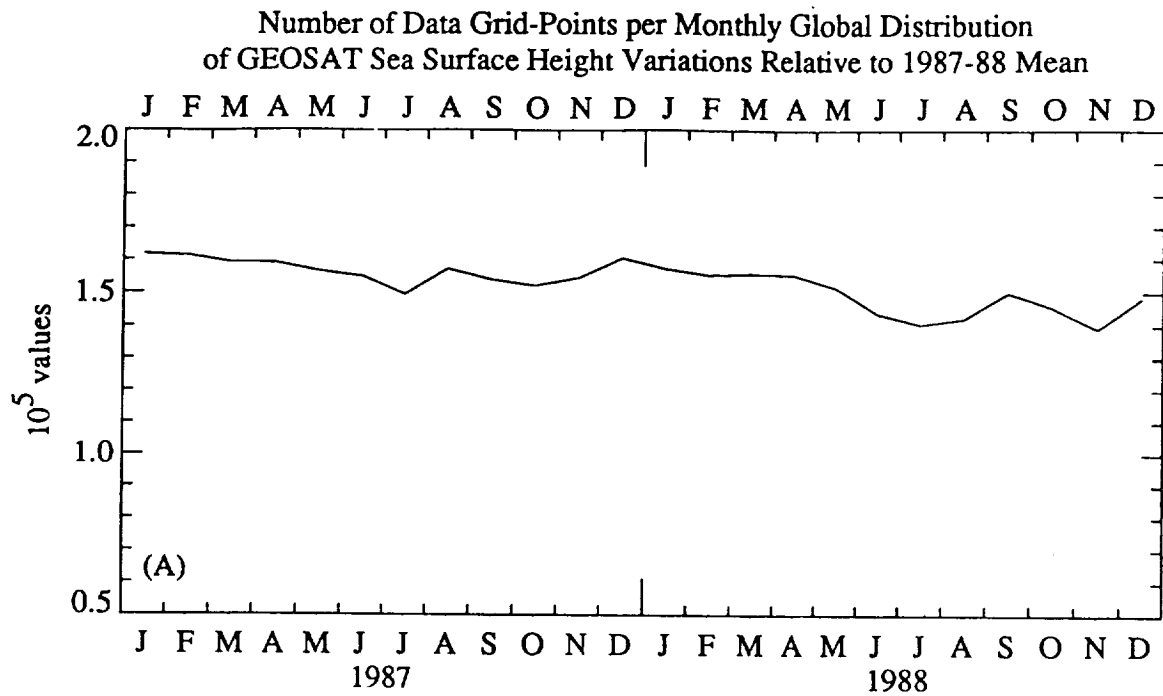Number of Data Grid-Points per Monthly Global Distribution
of GEOSAT Sea Surface Height Variations Relative to 1987-88 Mean

Total Number of Data Values per Monthly Global Distribution
of GEOSAT Sea Surface Height Variations Relative to 1987-88 Mean

Figure 2. Time series of monthly totals of (A) number of 1/3° x 1/3° pixels or picture elements and (B) number of sea surface height variations relative to a 2-year mean.

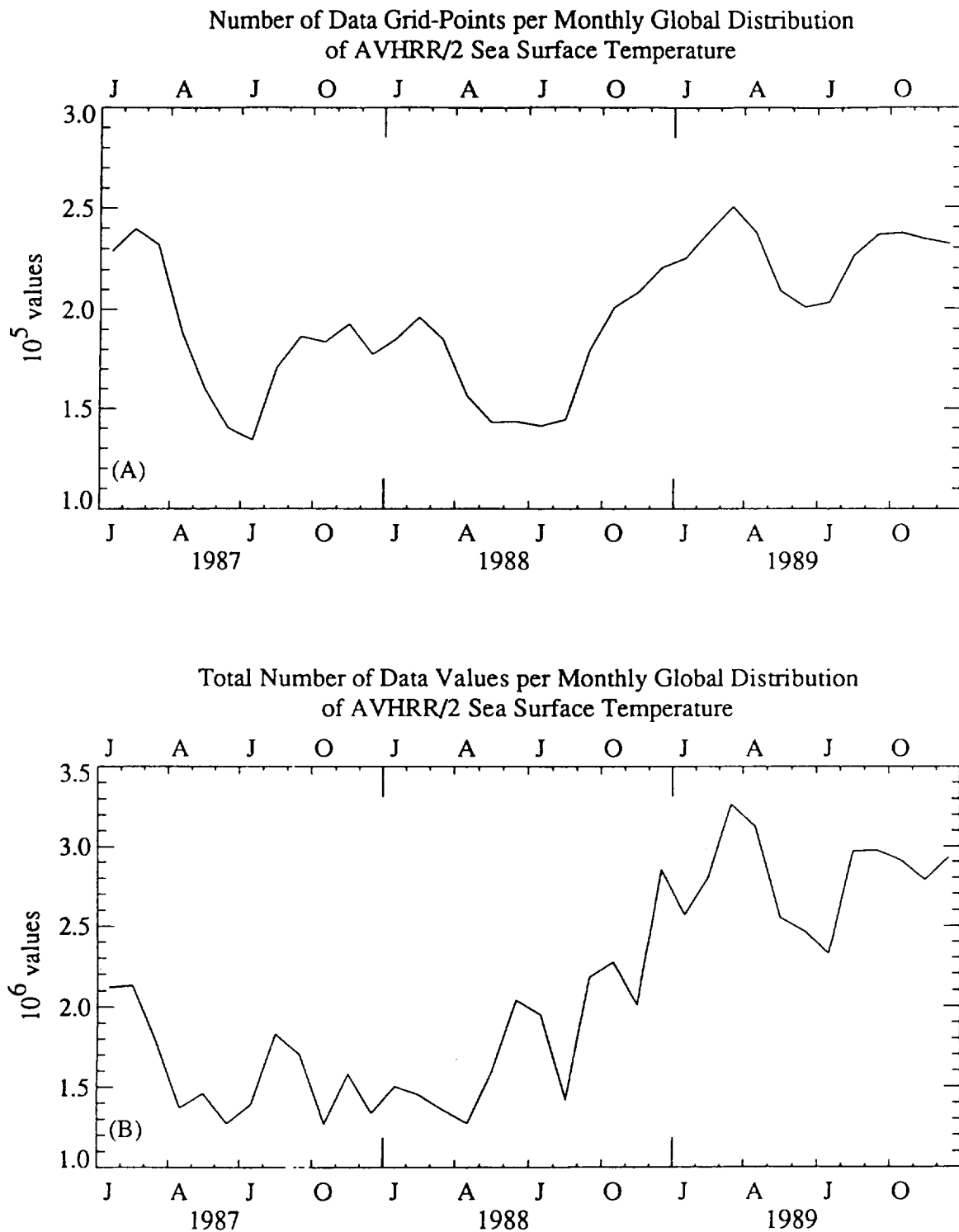## Number of Data Grid-Points per Monthly Global Distribution
of AVHRR/2 Sea Surface Temperature

Total Number of Data Values per Monthly Global Distribution
of AVHRR/2 Sea Surface Temperature

Figure 3. Time series of monthly totals of (A) number of 1/3° x 1/3° pixels or picture elements and (B) number of AVHRR/2 sea surface temperatures.